Huda JABER[1*] and Rasha SALMAN[1]

ELIMINATION OF MIXTURE OF DYES FROM SIMULATED WASTEWATER BY THREE-DIMENTIONAL ELECTRO-FENTON PROCESS: UTILISING ALUM SLUDGE AS A HETEROGENEOUS FENTON-LIKE CATALYST

Abstract: As a result of industrial development, many types of waste are generated, some of which are discharged into water, causing water pollution and having a negative impact on life. The electro-Fenton process (EF) has verified high efficiency in treating pollutants with low cost, ease of handling and operation, and this technology is one of the more efficient advanced oxidation technologies. The main objective of this present work is to explore the efficiency of a three-dimensional Electro-Fenton system (3DEF) in removing eosin, methylene blue, and methylene violet from simulated wastewater using graphite as anode, nickel foam as the cathode, and alum sludge as the third particle and as the source of catalyst. The study investigated the effect of operating parameters such as current density, *J*, catalyst concentration, and Na_2SO_4 concentration as supporting electrolyte, at a pH of 3, a temperature of (28 ±1) °C, an air flow rate of 20 L/h, and a treatment time of 30 minutes. Response surface methodology (RSM) was used to design and analyse experimental data. Based on the results of RSM, the best removal efficiency was achieved at J = 4.2 mA/cm^2, [Fe^{2+}] = 0.2 mM, and [Na_2SO_4] = 0.05 M, where the *Re* and chemical oxygen demand (COD) removal was 95.76 % and 100 %, respectively. The alum sludge was a very excellent choice as a primary source of Fe catalyst and the 3DEF process is an effective system that can eliminate many types of dyes.

Keywords: dyes, three-dimensional, electro-Fenton, alum sludge, surface response

Introduction

The accumulation of materials disposed of as industrial waste results in environmental pollution, both of which affects the land in general and of the water in particular, because most industries rely primarily on water in many of their stages, such as cooling [1] and dilution [2], or it may be used as a medium for various chemical [3] or physical [4] processes. Among these industries, the textile industry is considered one of the most polluting industries to the aquatic environment [5]. Colours, salt, total suspended solids (TSS), total dissolved solids (TDS), biological oxygen demand (BOD), and chemical oxygen demand (COD) are the main components released into the aquatic environment by textile industries [6].

Dyes differ in terms of their types, nature of use, properties, and chemical composition. There are acidic dyes, basic dyes, disperse dyes, direct dyes, reactive dyes, solvent dyes, sulphur dyes and Vat dyes [7]. Eosin yellowish, methylene blue and methylene violet dyes

[1] Department of Chemical Engineering, College of Engineering, University of Baghdad, Aljadria, Baghdad, Iraq, phone +9647735408870, ORCID: HJ 0009-0003-7144-2375, RS 0000-0001-9353-9096
[*] Corresponding author: huda.jaber2307m@coeng.uobaghdad.edu.iq

are among the most common dyes released from the textile industry into the aquatic environment, and are widely used in colouring cotton, silk, and paper. The concentration of these dyes in natural waters is approximately 0.1 μg to 130 μg for eosin [8], 0.05 μg to 80 μg for methylene blue [9], and for methylene violet the specific data of natural water is rare [10].

There are several techniques that have been used to purify wastewater from dye pollutants, like adsorption and coagulation [11], electrocoagulation [12, 13], biosorption [14], ozonation [15], membrane filtration [16], adsorption [17] and advanced oxidation [18, 19].

Each of the mentioned processes has different advantages and disadvantages, but the advanced oxidation process (AOPs) has shown advantages that make it the ideal choice for removing various pollutants from the aquatic environment by converting them into biodegradable organic compounds, inorganic ions, water and carbon dioxide, by means of hydroxyl radicals that are characterised by their easy productivity, high reactivity and selectivity [20]. The significant impact of electrochemistry on the treatment of refractory organic pollutants is their decomposition via active material generation, cathodic reduction or direct anodic oxidation. This is the basis upon which electrochemical processes of AOPs (EAOPs) are based [21]. EAOPs involves electrochemically generating hydrogen peroxide in the treated solution, favourably at a carbon cathode via the two-electron reduction of oxygen gas as shown in equation (1), and since the electro-Fenton process uses pure, pollution-free energy to instantly generate the oxidiser hydrogen peroxide and given the cost and risk of transporting this oxidiser, this process is widely used in wastewater treatment processes [22]:

$$O_{2g} + 2H^+ + 2e^- \rightarrow H_2O_2 \quad (1)$$

For many years, up until the end of the nineteenth century, researchers studied the oxidation mechanism of the normal Fenton process, which involves the reaction of hydrogen peroxide with an aqueous iron(II) salt. Hydroxyl radicals ($^{\cdot}OH$) are produced by the homogeneous Fenton reaction for the non-selective oxidation of many organic substances [23]. The main mechanism of the electro-Fenton process is the electrochemical production of hydrogen peroxide at a suitable cathode by adding iron(II) ions as a catalyst to the treated solution to reduce dissolved oxygen or air. The basic mechanism of the Fenton system is the production of one of the most effective oxidising agents ($^{\cdot}OH$) in the bulk solution. The subsequent Fenton chain of reactions begins with the homogeneous Fenton reaction as illustrated in equation (2), where the hydroxyl radical is produced by electron transfer through hydrogen peroxide and an iron catalyst, such as the iron(II) ion [24]:

$$Fe^{2+} + H_2O_2 \rightarrow Fe^{3+} + {}^{\cdot}OH + OH^-;\ k = 55.0\ M^{-1} \cdot s^{-1} \quad (2)$$

Fe^{2+} is added to an acidic solution at pH 3 to significantly improve the oxidising ability of the oxidising agent H_2O_2, forming OH_2, and Fe^{3+} as shown in equation [25]:

$$OH + H_2O_2 \rightarrow HO_2^- + H_2O \quad (3)$$

At the cathode, Fe^{3+} is reduced to Fe^{2+} through the reaction:

$$Fe^{3+} + HO_2^{\cdot} \rightarrow Fe^{2+} + H^+ + O_2 \quad (4)$$

$$Fe^{2+} + HO_2^{\cdot} \rightarrow Fe^{3+} + HO^{2-} \quad (5)$$

$$Fe^{2+} + {}^{\cdot}OH \rightarrow Fe^{3+} + OH^{-} \quad (6)$$

H_2O and O_2 are formed in the system because of the decomposition of hydrogen peroxide, with Fe^{3+} acting as a catalyst for this decomposition and replenishing the Fe^{2+} concentration, as shown in equations:

$$Fe^{3+} + H_2O_2 \leftrightarrow Fe\_O_2H^{2+} \leftrightarrow Fe^{2+} + HO_2^{\cdot} \quad (7)$$

$$Fe^{3+} + HO_2^{\cdot} \rightarrow Fe^{2+} + H^{+} + O_2 \quad (8)$$

The overall removal efficiency of organic compounds through coagulation is also improved by the action of both Fe^{2+} and Fe^{3+} as coagulants in the Fenton system [26].

Due to the high surface area per unit volume of carbonaceous electrodes; which provides a good space for reaction [27], they are widely used as anodes in wastewater treatment. Due to the low cost and high energy density, graphite is counted as an ideal anode [28]. Materials with good catalytic, absorption, and conductive properties are preferred in electrochemical systems used as cathodes, such as graphite felt (GF) [29], carbon felt [30], activated carbon fiber [31, 32], nickel foam and others. However, metal anodes in electro-Fenton systems can produce large amounts of metal salts, which increases subsequent processing costs [20].

In view of the many advantages of the nickel foam, such as its high electrical conductivity, and porous structure, and in addition to the fact that the accumulation of hydrogen peroxide at this electrode was higher compared to the graphite electrode, it was considered a workable alternative as a cathode, which leads to the formation of more ($^{\cdot}OH$) by producing more hydrogen peroxide in the system by generating oxygen gas on the surface of the electrode through the faster transfer of electrons through the electrode [33].

Recently, alum sludge (alum-based coagulants), extracted from water treatment and purification plants, which are composed of 30 % aluminium oxide and aluminium hydroxide deposits, is used as third particle and effective absorbents, removing various turbidity-causing contaminants and natural organic matter, and reducing colouration in wastewater treatment. This use of alum sludge is an effective strategy for recycling and reusing industrial waste, contributing to environmental sustainability and reducing water treatment costs [34]. Furthermore, adding alum sludge to the process and considering it the main source of the catalyst transforms the homogeneous two-dimensional electro-Fenton system into a heterogeneous three-dimensional EF system [35, 36].

In this work, the performance of EF process on the removal of mixture of the eosin, MB and MV dyes would be examined by applying Ni foam and porous graphite as the main electrodes in the EF and three-dimensional electro-Fenton systems assisted with alum sludge. The effect of different variables on the efficiency of these processes like alum sludge amount, current density, Fe^{2+} concentration and Na_2SO_4 concentration would be investigated.

Material and method

Chemicals

All chemicals had high purity, and distilled water was used to prepare aqueous solution. Table 1 shows the dyes which are used in this work, illustrates their properties and shows the chemical structure of these dyes. Sodium sulphate (Na_2SO_4) (Sisco Research Laboratories Pvt. Ltd., Ind.), hydrated iron sulphate ($FeSO_4 \cdot 7H_2O$) (Alpha Chemika, Ind.),

sulphuric acid (H_2SO_4) (SDFCL, Ind.), sodium hydroxide (NaOH) (Alpha Chemika, Ind.) were also used. The nickel foam is imported from Xiamen Top New Energy Technology Co., Ltd., China, graphite (from local market) and alum sludge from Karbala water treatment plant. A tintometer GmbH RD125 with SN 0214/5767, made in Germany by Dortmund Lovibond company, which work at 50 Hz - 60 Hz, device as a COD reactor for COD test was used.

Table 1

Dyes specification and chemical structure

Dye	Wavelength [nm]	Molecular weight [g·mol^{-1}]	Chemical structure
Eosin Y	516	691.85	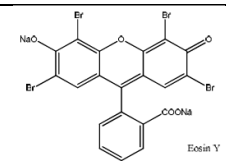
MB	690	319.85	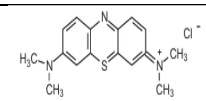
MV	580	407.99	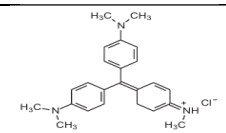

Experimental setup

A 1.0 L glass reactor was used for each batch run. It was filled with a 0.75 L of simulated wastewater consisting of distilled water and a 75 mg/L concentration of mixed dyes (25 mg/L for each Eosin, MB and MV dyes). Figure 1 shows the schematic drawing of the electro-Fenton process. The glass reactor covered with 10 mm thick Perspex plate with two holes for fitting of electrodes. Nickel foam plate (9 mm × 60 mm × 140 mm) was utilised as cathode and graphite (2 mm × 60 mm × 140 mm) as anode, and with distance of 3 cm was fixed between them. The reaction mixture was continuously mixed with 300 rpm by magnetic stirrer (Stu art CD-162, Biocote). Before each run the nickel foam washed with 0.1 M of H_2SO_4 solution and deionised water to clean the surface of the electrode from all residual impurities and dried at 80 °C for several hours in dryer [36]. The graphite was thermally activated for 30 min at 350 °C [37].

To ensure the continued availability of oxygen in the reaction mixture, it aerated with air continuously by pumped air in using a pump (HAILEA, model ACO-208, China) at a flow rate of 20 L/h. The aqueous solution was aerated for 20 minutes before switching the DC supply. The best environment for the EF reaction is the acidity and for adjusting the reaction mixture pH at 3, the solution of 0.1 M H_2SO_4 and NaOH was used [26]. To support and improve the conductivity of the electrolyte the Na_2SO_4 added with different concentrations [38]. The voltage was supplied by DC power supply (MAISHENG MS-605D), which is used to supply the current to the EF system. The reaction required a desired value of Fe^{2+} to enhanced the oxidising ability of H_2O_2 [26], and that provided by adding the catalyst ($FeSO_4 \cdot 7H_2O$) to the mixture. All experiments were run at ambient

temperature, and each run was duplicated, and average value was adopted. Alum sludge was prepared by forming cylindrical particles with 0.5 cm in long and 0.3 cm in diameter and then dried at 80 °C for 24 hours and then calcined at 300 °C for 30 minutes [34]. The UV-9200 spectrometer was used to determine the dye mixture concentrations, and the removal efficiency, *Re* [%], was determined by equation [39, 40]:

$$Re = \frac{C_0 - C_f}{C_0} \cdot 100 \tag{9}$$

where C_0 is initial concentration [mg/L] and C_f of dyes.

The Chemical Oxygen Demand (COD) was measured at optimum conditions to detect the removal of organic not only colour by Lovibond reactor (tintometer GmbH RD125 with SN 0214/5767, Germany). Equation (10) was utilised to obtain the specific energy consumption, *SEC* [kWh/kg_{dye}] [41].

$$SEC = \frac{J \cdot U \cdot 1000}{\Delta c \cdot v} \tag{10}$$

where J is current density [mA/cm^2], Δc is concentration difference [mg/L], U is voltage [V], and v is volume of the reaction solution [L].

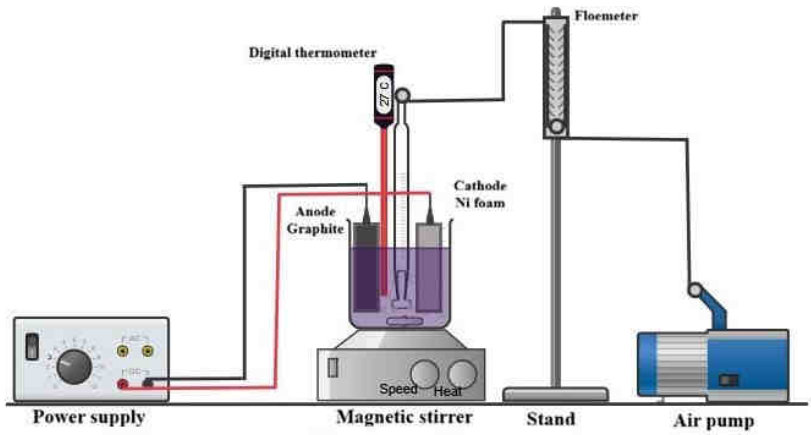

Fig. 1. The schematic diagram of electro-Fenton process

Design of experiment

The functional relationship between response and a set of influencing variables can be approximated using a set of statistical methods known as the Box-Behnken design (BBD). This experimental design is often used to optimise various processing operations. It can also be used to study the combined effect of different variables on response, which in turn improves multifactorial processes [42]. In this study, using Box-Behnken experimental Design (BBD), three factors at three levels that control the removal of dye mixtures from the pollutant water were investigated. Table 2 illustrates these parameters and their range, and Table 3 shows the design of the BBD of this study. Where $X1$, $X2$ and $X3$ were current density, $FeSO_4 \cdot 7H_2O$ and Na_2SO_4 respectively, and the total removal efficiency were the response of this study. To analyse the result of dye mixture removal efficiency the Minitab-22 software was used.

Table 2

The process variables and their levels for dye mixture removal efficiency

Variables	Units	Sample	Low (–1)	Middle (0)	High (+1)
Current density	[mA/cm^2]	*X*1	1.40	2.80	4.20
$FeSO_4 \cdot 7H_2O$	[mM]	*X*2	0.10	0.15	0.20
Na_2SO_4	[M]	*X*3	0.01	0.03	0.05

Table 3

BBD design for dye mixture removal efficiency

Run	Coded values			Real values		
	*X*1	*X*2	*X*3	Current density [mA/cm^2]	$FeSO_4 \cdot 7H_2O$ [mM]	Na_2SO_4 [M]
1	–1	0	+1	1.4	0.15	0.05
2	0	–1	+1	2.8	0.10	0.05
3	0	0	0	2.8	0.15	0.03
4	+1	–1	0	4.2	0.10	0.03
5	0	+1	+1	2.8	0.20	0.05
6	0	0	–1	2.8	0.20	0.01
7	0	0	0	2.8	0.15	0.03
8	0	–1	–1	2.8	0.10	0.01
9	–1	+1	0	1.4	0.20	0.03
10	+1	+1	0	4.2	0.20	0.03
11	0	0	0	2.8	0.15	0.03
12	–1	–1	0	1.4	0.10	0.03
13	–1	0	–1	1.4	0.15	0.01
14	+1	0	+1	4.2	0.15	0.05
15	+1	0	–1	4.2	0.15	0.01

Ni foam and alum sludge characterisation

The elemental composition of the Ni foam and alum sludge was determined using Energy Dispersive X-ray Spectroscopy (EDX), and the surface morphology of alum sludge was observed with scanning electron microscopy (SEM) (model Axia ChemiSEM).

Result and discussion

Static analysis

The Minitab-22 software was used to attain a quadric equation (equation (11)) which calculates the efficiency of dye mixture removal and clarifies the relationship between *Re* and the parameters studied. Table 4 illustrates the actual *Re* of dyes based on the BBD and the predicted *Re* which was determined based on equation:

$$Re = 59.43 - 228.5 \cdot [Fe^{2+}] + 247 \cdot [Na_2SO_4] + 14.61 \cdot J + 889 \cdot [Fe^{2+}] \cdot [Fe^{2+}] + 8022 \cdot [Na_2SO_4] \cdot [Na_2SO_4] - 0.998 \cdot J \cdot J - 681 \cdot [Fe^{2+}] \cdot [Na_2SO_4] + 8.71 \cdot [Fe^{2+}] \cdot J - 127.9 \cdot [Na_2SO_4] \cdot J \quad (11)$$

As shown in Table 4, the *Re* range was 66.00 % - 95.76 % which are represented by the runs (13) and (10) respectively, and the *SEC* range was from 1.00 kWh/kg$_{dye}$ to 8.52 kWh/kg$_{dye}$ as shown by runs (1) and (15). When comparing the result of two runs (13) and (15), it appears that the effect of current density on removal efficiency was vital. Dye mixture removal efficiency increased from 66.00 % to 89.87 % when the current density

increased from 1.4 mA/cm^2 to 4.2 mA/cm^2 with constant concentrations for both $FeSO_4 \cdot 7H_2O$ and Na_2SO_4 at 0.15 mM and 0.01 M, respectively. While the comparison between run (13) and (1) shows that the *Re* increased from 66.00 % to 85.30 % with different 19.3 % in *Re* when the Na_2SO_4 concentration increased from 0.01 M to 0.05 M with constant concentration of $FeSO_4 \cdot 7H_2O$ at 0.15 mM and current density at 1.4 mA/cm^2. This illustrates that the Na_2SO_4 concentration had the second effluence on dye mixture removal efficiency in this work. In addition, the *Re* increased from 89.94 % to 95.76 % as $FeSO_4 \cdot 7H_2O$ concentration increased from 0.1 mM to 0.2 mM with a constant value of current density at 4.2 mA/cm^2 and Na_2SO_4 concentration at 0.03 M.

Table 4

Obtained actual and predicted removal efficiency of the dye mixture and the energy consumption of the process

Run	Current density [mA/cm^2]	$FeSO_4 \cdot 7H_2O$ [mM]	Na_2SO_4 [M]	Actual *Re* [%]	Predicted *Re* [%]	Voltage [V]	*SEC* [kWh/kg$_{dye}$]
1	1.4	0.15	0.05	85.30	83.86	1.90	1.00
2	2.8	0.10	0.05	91.60	92.12	2.40	2.35
3	2.8	0.15	0.03	82.53	82.75	2.70	2.93
4	4.2	0.10	0.03	89.94	89.75	1.24	1.85
5	2.8	0.20	0.05	94.10	94.99	2.60	2.48
6	2.8	0.20	0.01	86.13	85.61	3.90	4.06
7	2.8	0.15	0.03	82.95	82.75	2.90	3.13
8	2.8	0.10	0.01	80.91	80.02	5.20	5.76
9	1.4	0.20	0.03	74.88	75.43	2.20	1.32
10	4.2	0.20	0.03	95.76	94.84	3.70	5.19
11	2.8	0.15	0.03	82.78	82.75	3.20	3.46
12	1.4	0.10	0.03	71.50	72.42	2.50	1.57
13	1.4	0.15	0.01	66.00	65.97	3.10	2.10
14	4.2	0.15	0.05	94.85	94.88	2.70	3.83
15	4.2	0.15	0.01	89.87	91.31	5.70	8.52

This result showed that all the studied factors (*J*, Fe^{2+} conc., and Na_2SO_4 conc.) were all effective in the process of dye removal. But the greatest effect of current density was clear, as the removal efficiency is directly proportional to this factor, and the next factor that influences *Re* is the Na_2SO_4 concentration. The result showed that the increasing electrolyte concentration leads to increasing in the removal efficiency in this study.

ANOVA analysis

Experimental conditions can be classified according to the factors number used in the study, with two or more levels for each factor, using a general linear model used in factorial designs generally, such as ANOVA analysis of variance [43]. The importance of the coefficient terms can be implied by estimating the significance of the model and its parameters, which can be done by the analytical method with response surface mythology by *F* (Fishers)-test and *P*-test. Generally high *F*-value (> 4) and a low *P*-value (< 0.05) illustrate this importance [44, 45]. Based on the results of the response surface methodology illustrated in Table 5, the current density with cont. % 62.16 denotes its main impact on dye removal efficiency. The significance of Na_2SO_4 concentration was 21.66 contr. % while the $FeSO_4 \cdot 7H_2O$ concentration with contr. % 3.36 had a lower effect on the dye mixture removal efficiency compared with the other factors in this study. Based on *P*-value result for the model (0.000 < 0.050), high *F*-value (381.62 > 4), and high multiple correlation

coefficient (R^2) value for the model (99.19), the statistical significance of the regression can be confirmed.

Table 5

ANOVA analysis for dye mixture removal

Source	DF	Seq ss	Contr.%	Adj SS	Adj MS	*F*-value	*P*-value
Model	9	1055.30	99.19	1055.30	117.256	67.66	0.000
Linear	3	927.64	87.19	927.64	309.212	178.42	0.000
$FeSO_4{\cdot}7H_2O$	1	35.80	3.36	35.80	35.798	20.66	0.006
Na_2SO_4	1	230.45	21.66	230.45	230.448	132.97	0.000
J	1	661.39	62.16	661.39	661.388	381.62	0.000
Square	3	73.06	6.87	73.06	24.354	14.05	0.007
$FeSO_4{\cdot}7H_2O \cdot FeSO_4{\cdot}7H_2O$	1	17.01	1.60	18.26	18.254	10.53	0.023
$Na_2SO_4{\cdot}Na_2SO_4$	1	41.91	3.94	38.02	38.015	21.93	0.005
$J \cdot J$	1	14.14	1.33	14.14	14.142	8.16	0.036
2-way interaction	3	54.61	5.13	54.61	18.203	10.50	0.013
$FeSO_4{\cdot}7H_2O \cdot Na_2SO_4$	1	1.85	0.17	1.85	1.854	1.07	0.348
$FeSO_4{\cdot}7H_2O \cdot J$	1	1.49	0.14	1.49	1.488	0.86	0.397
$Na_2SO_4 \cdot J$	1	51.27	4.82	51.27	51.266	29.58	0.003
Error	5	8.67	0.81	8.67	1.733	-	-
Lack-of-fit	3	8.58	0.81	8.58	2.859	64.05	0.015
Pure error	2	0.09	0.01	0.09	0.045	-	-
Total	14	1063.97	100.00	-	-	-	-
Model summary	**S**	**R^2 [%]**	**R^2 (adj.) [%]**	**Press**	**R^2 (pred.) [%]**	-	-
	1.31647	99.19	97.72	137.420	87.08	-	-

Effect of studied factors on dye *Re*

The interactions between operational factors on dye removal efficiency can be studied more comprehensively by using two-dimensional plots and three-dimensional response surfaces, as shown in Figure 2.

Figure 2 (a1 and b1) illustrate the current density effect at different concentrations of Na_2SO_4 and fixed concentration of $FeSO_4{\cdot}7H_2O$ at 0.15 mM. The surface plot and 2D plot show a direct relationship between the current density and the removal efficiency, and a noticeable increase in *Re* can be noticed as the current density increases, which indicates the significant effect of the current on improving the removal of pollutants. Whereas the mA/cm^2 where the removal rate appears in the ninety percent range. And that agree with [46] which showed that the rising in current density led to rising the removal efficiency of methyl orange, the *J* range used in this work was from 3 mA/cm^2 to 8 mA/cm^2, and the *Re* range was from 54.86 % to 97.60 %, and also agrees with [47]. The direct correlation between current and removal can be explained by the fact that increasing the current leads to an acceleration of electron movement, meaning an increase in hydrogen peroxide production and consequently an increase in hydroxyl radical generation, thus improving the oxidation process of pollutants in water. This results in an increase in the removal efficiency [36].

Figure 2 (a2 and b2) show the effect of the Na_2SO_4 concentration factor on removal efficiency with different concentrations of $FeSO_4{\cdot}7H_2O$ and a fixed current density value at

2.8 mA/cm^2, as the increase in electrolyte concentration is directly proportional to the *Re*. It is noted that with the increase in Na_2SO_4 concentration, there is an increase in the removal rate, and that consistent with [48] which found that the dimethyl phthalate removal rate is good at a 0.05 M of electrolyte concentration, as this enhances the electrical conductivity of the system.

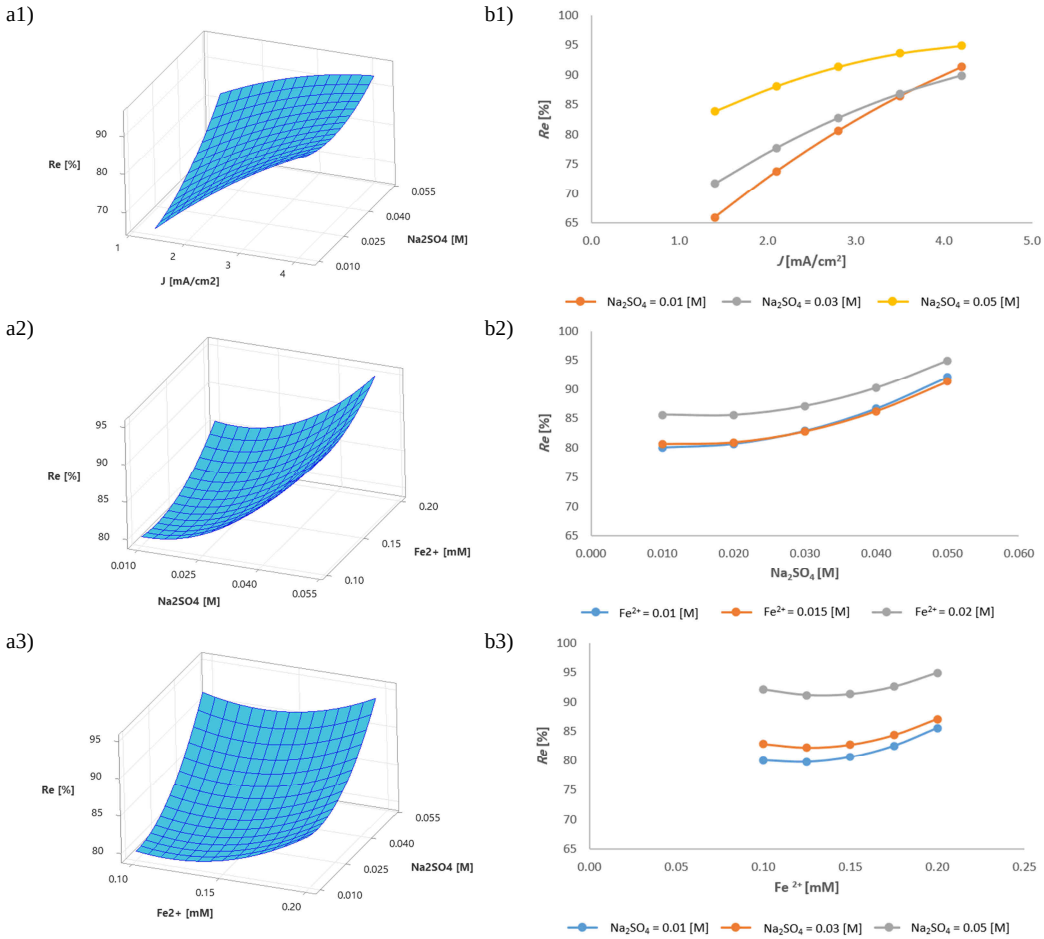

Fig. 2. a1) 3D plot, b1) 2D plot for dye mixture *Re* at $FeSO_4 \cdot 7H_2O$ = 0.15 mM, and different concentrations of Na_2SO_4 and current density, a2) 3D plot, b2) 2D plot for dye mixture *Re* at current density = 2.8 mA/cm^2, and different concentrations of Na_2SO_4 and $FeSO_4 \cdot 7H_2O$, and a3) 3D plot, b3) 2D plot for dye mixture *Re* at *J* = 2.8 mA/cm^2, and different concentrations of $FeSO_4 \cdot 7H_2O$ and Na_2SO_4

Figure 2 (a3 and b3) clarify the $FeSO_4 \cdot 7H_2O$ concentration with different concentrations of electrolyte and fixed values of current density at 2.8 mA/cm^2. The figure shows the slight effect of changing the concentration of the catalyst ($FeSO_4 \cdot 7H_2O$) on the removal rate compared to the previous two factors, i.e. current density and Na_2SO_4

concentration. As mentioned previously in the analysis of the results, it can be said that the concentration of the catalyst does not have a clear effect on improving the removal efficiency in this work.

Adding Na_2SO_4 improves the conductivity of the system, meaning it increases the flow rate of electrons through the cell. This, of course, results in increased oxygen release at the anode, and consequently, an increased rate of hydrogen peroxide production, which enhances the Fenton reaction as the hydroxyl radical production is increased. But, with excess concentration of Fe^{2+}, Hydrogen peroxide reacts with Fe^{2+} to form hydroperoxide radicals ($OH_2^{\cdot}$), which is a weaker oxidising agent than $^{\cdot}OH$, as mentioned in equation 7. This means consuming hydrogen peroxide instead of reacting to produce a $^{\cdot}OH$, thus decay the Fenton reaction and as a result reducing the *Re* [49]. Therefore, the higher concentration of Fe^{2+}, i.e. 0.2 mM, used in this procedure was appropriate for the process and within limits that ensured the process progressed towards satisfactory removal.

The optimisation and confirmation test

The optimal removal values of operating factors, i.e. *J*, $FeSO_4{\cdot}7H_2O$ and Na_2SO_4, according to the analysis predicted by the Minitab-22 software and according to the BBD design, are shown in Table 6. The obtained removal result was within the program's predicted limits, as shown in Table 7. The results obtained prove that the program used in MiniTab-22 was a statistical mand model-based for designing this process. At these optimum conditions, COD was measured at the beginning and after experiment, and these values were 19 mg/L and 0 mg/L, respectively. These COD values indicate that there was a decrease in organic content not only in colour.

Table 6

Optimal system variable performance for maximum dye mixture removal

Response	**Goal**	**Lower**	**Target**	**Upper**	**Weight**	**Importance**
Dye mixture *Re*	maximum	66.00 %	95.76 %		1	1
Parameter solution			**Multiple response prediction**			
J [mA/cm^2]	$FeSO_4{\cdot}7H_2O$ [mM]	Na_2SO_4 [M]	*Re* fit. [%]	95 % CI	95 % PI	Composite desirability
4.2	0.2	0.05	99.15	95.15	93.91	1

Table 7

Confirmation experiments of dye mixture removal

Run	***J*** **[mA/cm^2]**	**$FeSO_4{\cdot}7H_2O$ [mM]**	**Na_2SO_4 [M]**	***U*** **[V]**	***SEC*** **[kWh/kg$_{dye}$]**	***Re*** **[%]**	**Average *Re* [%]**
1	4.20	0.20	0.05	3.70	5.35	93.00	94.05
2	4.20	0.20	0.05	3.90	5.51	95.10	

Alum sludge effect

To demonstrate the effect of alum sludge, the experiment, which showed the lowest *Re*, i.e. run (13) with 66.00 %, was repeated with the addition of alum sludge in the solution with different concentrations, 5 g/L, 10 g/L, 15 g/L and 20 g/L as illustrated in Figure 3a.

The addition of calcined alum sludge at 300 °C resulted in a significant change and improvement in the removal efficiency of the dye mixture, with 78.8 % removal when

adding only 5 g/L of alum sludge and 98.16 % removal when adding 20 g of alum sludge per litre of the dye mixture, as shown in Table 8. This can be attributed to the alum sludge acting as a third electrode in the EF process during the current flow, as it contains different metals and oxides in its composition, which will be mentioned next, according to EDX tests.

a)

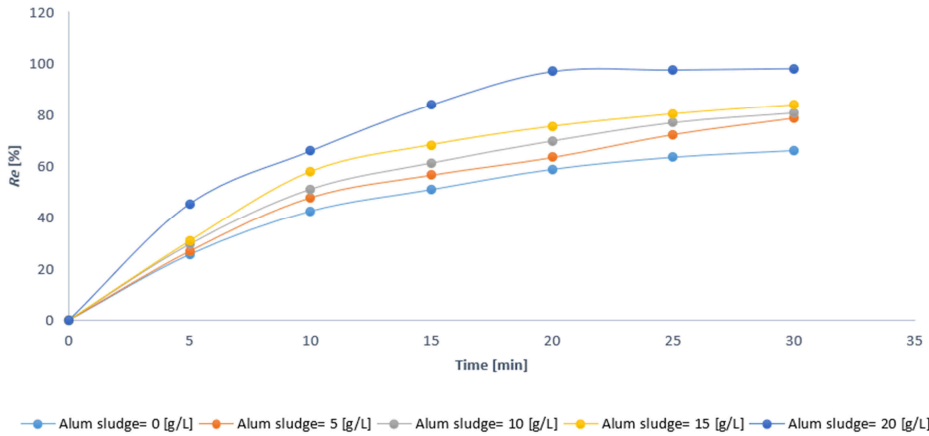

b)

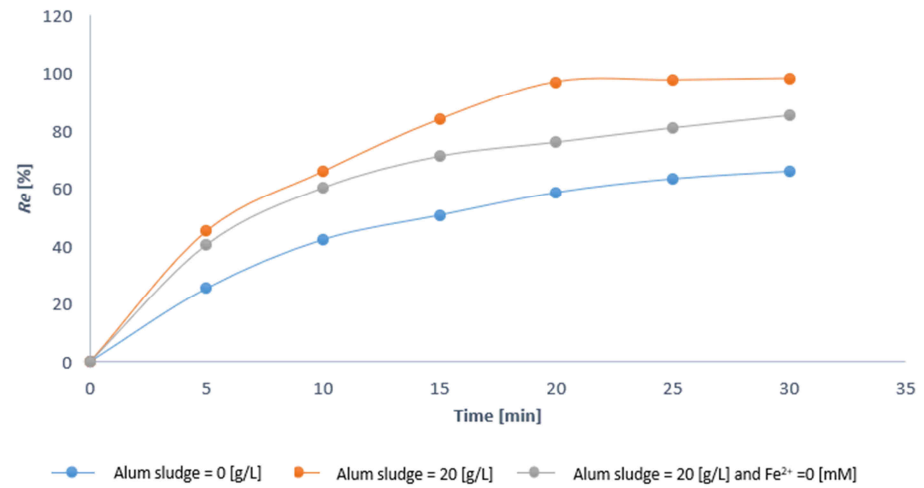

Fig. 3. a) Removal efficiency in presence of different concentrations of alum sludge, b) Removal efficiency in presence of 0 g/L, 20 g/L of alum sludge and 20 g/L alum sludge with 0 mM of $FeSO_4 \cdot 7H_2O$

In addition to the adsorption capacity of alum sludge [34], it contains iron(II) oxide, which is considered the main catalyst for the Fenton reaction, which greatly helped to improve removal efficiency. Therefore, the reaction was tested without adding $FeSO_4 \cdot 7H_2O$, with a concentration of 20 g/L of alum sludge, as it showed the highest

removal result under the worst operating conditions of the process run (13). The results, as shown in Figure 3b, showed that the *Re* was 85.05 %, i.e. a difference of 11.95 % from the experiment in which $FeSO_4 \cdot 7H_2O$ was added as a catalyst. The difference in the removal percentage was 19.05 % compared to the run (13), which is considered a not insignificant difference in removal efficiency, and this indicates that the amount of Fe^{2+} present in the clay was sufficient. Therefore, it is possible to consider alum sludge a sufficient source of catalyst, i.e. Fe^{2+}, for this process [48, 49], and Figure 4a illustrates the EDX of alum sludge which emphasise the presence of Fe in its structure, while Figure 4b shows the high porosity of its surface.

Table 8

Repeated run (13) at J = 1.4 mA/cm^2, $FeSO_4 \cdot 7H_2O$ = 0.15 mM, and Na_2SO_4 = 0.01 M

Alum sludge [g/L]	***Re* [%]**	***U* [V]**	***SEC* [kWh/kg$_{dye}$]**	**Diff. in *Re* [%]**
5	78.80	3.3	1.88	12.80
10	80.70	3.2	1.78	14.67
15	83.88	2.9	1.55	17.85
20	98.16	2.9	1.32	32.13

a) b)

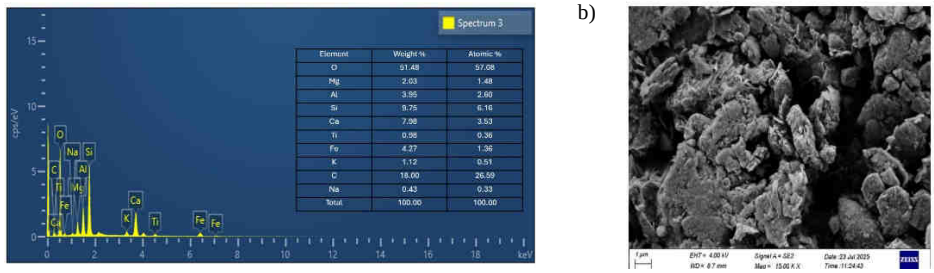

Fig. 4. a) EDX of alum sludge, b) SEM of alum sludge

Ni foam characterisation and leaching

Figure 5a shows the EDX of the Ni electrode, and it emphasises that the electrode has high purity. Increasing the efficiency of Fenton reagent production depends largely on the surface area available for the reaction, which is provided by the Ni electrode surface with a high surface area. By improving the conductivity and specific surface area of the cathode, the removal of dye contaminants is improved by increasing the production of hydroxyl radicals. Figure 5b shows the EDX of Ni foam which is displaying and determining the elemental composition of the Ni foam after the reaction, which indicates the presence of carbon and oxygen in the structure of the electrode, and this improve that the C and O are presented in aqueous solution as a result of reactions and C is released from anode and these elements precipitated on the surface of Ni foam which decreased its percentage and this was approved by measuring the Ni ion concentration in solution which was lower than 1 mg/L. The highest permissible concentration of Ni in released industrial waste and drinking water is 2 mg/L and 0.1 mg/L, respectively, according to World Health Organisation (WHO) guidelines [50]. Therefore, it is a vital issue to detect its concentration in the treated solution and based on the results of the present study it was within the limitations of WHO. Consequently, the studied system can be operated to obtain a good percentage of dye removal efficiency with an acceptable concentration of Ni ions [50].

a)

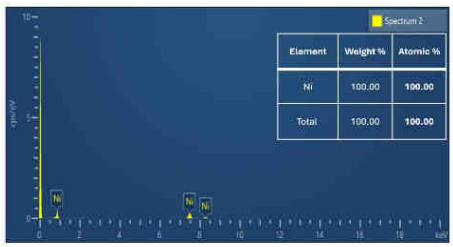

b)

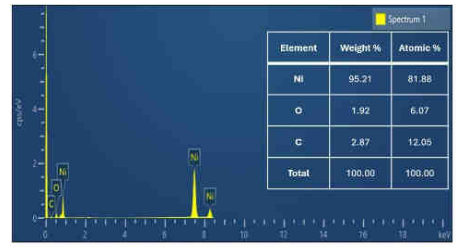

Fig. 5. a) EDX of Ni foam before using as a cathode in Ef process, b) EDX of Ni foam after using as cathode in EF process

Conclusion

Three levels of Box-Behnken design were used to design and optimise the removal of a mixture of dyes (Eosin, MB and MV) with three variables, current density, $FeSO_4 \cdot 7H_2O$ and Na_2SO_4. Ni foam and graphite were used as the cathode and anode respectively. Ni foam provides high surface area due to its structure, which enhances the removal efficiency for dyes. The P and F-values were used to confirm the validity of the model which showed the significant overall acceptability model. The optimum condition, with is 95.76% and 100% removal efficiency and COD removal, respectively, was acquired at 4.2 mA/cm^2 of *J*, 0.2 mM of $FeSO_4 \cdot 7H_2O$ and 0.05 M of Na_2SO_4 concentrations. The current density has the main effect on the efficiency of the process based on ANOVA result and the Ni foam was efficient as a cathode. Given the effectiveness of alum sludge in improving removal under the worst conditions and providing a sufficient quantity of catalyst for the Fenton reaction, it can be considered a promising method for wastewater management. This undoubtedly achieves integration between various industrial processes on the one hand and reduces the cost of treating polluted water on the other, since alum sludge is a waste and does not require a specific manufacturing cost. Furthermore, considering the high treatment or pollutant removal rates achieved by the electro-Fenton process at acceptable costs, does not require high current amounts, which results in energy conservation in the long orbit, along with its ease of operation and safety in handling materials, this process can be considered promising for practical application in water treatment plants.

References

[1] Peixing L, Feng Ch, Ke Sh, Weiguo L. Water jacket and slot optimization of a water-cooling permanent Magnet synchronous in-wheel motor. IEEE Trans Ind Appl. 2021;57(3):2431-9. DOI: 10.1109/TIA.2021.3064779.

[2] Qun W, Xueli G, Yushan Z, Jian W, Yuan X, Zhiyong J, et al. Alleviation of water flux decline in osmotic dilution by concentration-dependent hydraulic pressurization. Chem Eng Res Des. 2017;117:593-603. DOI: 10.1016/j.cherd.2016.11.023.

[3] Rana K, Şifa D. Medium-high frequency ultrasound and ozone based advanced oxidation for amoxicillin removal in water. Ultrason Sonochem. 2018;40:131-9. DOI: 10.1016/j.ultsonch.2017.01.033.

[4] Claude AF, Oh SP. Key physical processes in the circumgalactic medium. Annu Rev Astron Astrophys. 2023;61:131-95. DOI: 10.1146/annurev-astro-052920-125203.

[5] Ali H, Lynn P. A technical review of emerging technologies for energy and water efficiency and pollution reduction in the textile industry. J Clean Prod. 2015;95:30-44. DOI: 10.1016/j.jclepro.2015.02.079.

[6] Teshale A, Amare TA, Esayas A. Textile industry effluent treatment techniques teshale. J Chem. 2021:5314404. DOI: 10.1155/2021/5314404.

[7] Gupta VK, Suhas. Application of low-cost adsorbents for dye removal - A review. J Environ Manage. 2009;90(80):2313-42. DOI: 10.1016/j.jenvman.2008.11.017.
[8] Kakalejčíková S, Bazel Y, Drábiková M, Fizer M. Fluorimetric determination of eosin Y in water samples and drinks using deep eutectic solvent-based liquid-phase microextraction. Molecules. 2025;30(16):3334. DOI: 10.3390/molecules30163334.
[9] Tkaczyk-Wlizło A, Mitrowska K, Błądek T. Quanti fi cation of twenty pharmacologically active dyes in water samples using UPLC-MS / MS. Heliyon. 2022;8:e09331. DOI: 10.1016/j.heliyon.2022.e09331.
[10] Al-zaban MI, Alharbi NK, Albarakaty FM, Alharthi S, Sedky HAH, Mustafa AF. Experimental modeling investigations on the biosorption of methyl violet 2B dye by the brown seaweed cystoseira tamariscifolia. Sustainability. 2022;14. DOI: 10.3390/su14095285.
[11] Kiattisaksiri P, Noppakhun P. Combination of coagulation and VUV+H_2O_2 for the treatment of color and organic matter in treated effluent wastewater from a sugar factory. Appl Sci Eng Progress. 2023. DOI: 10.14416/j.asep.2022.08.002.
[12] Shahedi A, Darban AK, Taghipour F, Jamshidi-Zanjani A. A review on industrial wastewater treatment via electrocoagulation processes. Curr Opin Electrochem. 2020;22:154-69. DOI: 10.1016/j.coelec.2020.05.009.
[13] Al-Jubouri SM, Salman RH, Entisar MK, Abbas AS, Al-Alawy AF, Sajad YK, et al. Multicomponent equilibrium isotherms and kinetics study of heavy metals removal from aqueous solutions using electrocoagulation combined with mordenite zeolite and ultrasonication. Appl Sci Eng Process. 2025;18(1):7484. DOI: 10.14416/j.asep.2024.07.011.
[14] Al-Mashhadani ESM, Al-Mashhadani MKH, Al-Maari MA. Biosorption of ciprofloxacin (CIP) using the waste of extraction process of microalgae: The equilibrium isotherm and kinetic study. Iraqi J Chem Petrol Eng. 2023;24(4):1-15. DOI: 10.31699/IJCPE.2023.4.1.
[15] Supitchaya J, Sumana S, Thunyalux R. Performance and pathway of 4-chloroaniline degradation: A comparative study of electro-peroxone, ozonation, and electrolysis processes. Appl Sci Eng Process. 2025;19(1):7777. DOI: 10.14416/j.asep.2025.05.009.
[16] Alkarbouly SM, Basma IW. Fabrication of electrospun nanofibers membrane for emulsified oil removal from oily wastewater. Baghdad Sci J. 2022;19(6):1238-48. DOI: 10.21123/bsj.2022.6421.
[17] Muthanna JA. Adsorption of non-steroidal anti-inflammatory drugs from aqueous solution using activated carbons: Review. J Environ Manage. 2017;190:274-82. DOI: 10.1016/j.jenvman.2016.12.073.
[18] Baybars AF, Mustafa K, Cengiz Ö. Application of nonlinear regression analysis for methyl violet (MV) dye adsorption from solutions onto illite clay. J Dispers Sci Technol. 2016;37(7):991-1001. DOI: 10.1080/01932691.2015.1077455.
[19] Lokesh KA, Raj KO, Debraj B. Treatment of marigold flower processing wastewater using a sequential biological-electrochemical process. Appl Sci Eng Process. 2021;14(3):525-42. DOI: 10.14416/j.asep.2021.04.001.
[20] Dongbao S, Junfeng L, Zhaoyang W, Chun Z. Performance of graphite felt as anodes in the electro-Fenton oxidation systems: Changes in catalysis, conductivity and adsorption properties. Appl Surf Sci. 2020;532:147450. DOI: 10.1016/j.apsusc.2020.147450.
[21] Dakhil IH, Abbas AS. Challenges and future directions in photoelectro-Fenton techniques: A comprehensive review of emerging applications and innovations. Iraqi J Chem Petrol Eng. 2025;26(3):63-83. DOI: 10.31699/IJCPE.2025.3.7.
[22] Buftia G, Rosales E, Pazos M, Lazar G, Sanromán MA. Electro-Fenton process for implementation of acid black liquor waste treatment. Sci Total Environ. 2018;635:397-404. DOI: 10.1016/j.scitotenv.2018.04.139.
[23] Umar M, Aziz HA, Yusoff MS. Trends in the use of Fenton, electro-Fenton and photo-Fenton for the treatment of landfill leachate. Waste Manage. 2010;30(11):2113-21. DOI: 10.1016/j.wasman.2010.07.003.
[24] Babuponnusami A, Muthukumar K. Advanced oxidation of phenol: A comparison between Fenton, electro-Fenton, sono-electro-Fenton and photo-electro-Fenton processes. Chem Eng J. 2012;183:1-9. DOI: 10.1016/j.cej.2011.12.010.
[25] Bedolla-Guzman A, Sirés I, Thiam A, Peralta-Hernández JM, Gutiérrez-Granados S, Brillas E. Application of anodic oxidation, electro-Fenton and UVA photoelectro-Fenton to decolorize and mineralize acidic solutions of reactive Yellow 160 azo dye. Electrochim Acta. 2016;206:307-16. DOI: 10.1016/j.electacta.2016.04.166.
[26] He H, Zhou Z. Electro-Fenton process for water and wastewater treatment. Crit Rev Environ Sci Technol. 2017;47(21):2100-31. DOI: 10.1080/10643389.2017.1405673.
[27] Zhang H, Yang Y, Ren D, Wang L, He X. Graphite as anode materials: Fundamental mechanism, recent progress and advances. Energy Storage Mater. 2021;36:147-70. DOI: 10.1016/j.ensm.2020.12.027.
[28] Ghjair AY, Abbar AH. Removal of chemical oxygen demand (COD) from hospital wastewater by electro fenton process using graphite-graphite electrochemical system. Al-Qadisiyah J Eng Sci. 2022;15(1):23-31. DOI: 10.30772/qjes.v15i1.809.

[29] Panizza M, Oturan MA. Degradation of Alizarin red by electro-Fenton process using a graphite-felt cathode. Electrochim Acta. 2011;56(20):7084-7. DOI: 10.1016/j.electacta.2011.05.105.
[30] Petrucci E, Pozzo AD, Palma LD. On the ability to electrogenerate hydrogen peroxide and to regenerate ferrous ions of three selected carbon-based cathodes for electro-Fenton processes. Chem Eng J. 2016;283:750-8. DOI: 10.1016/j.cej.2015.08.030.
[31] Chun Z, Bin S, Zakaria AM, Yuanyuan L, Xinlin H, Jungeng L, et al. Activated carbon fiber (ACF) enhances the UV/EF system to remove nitrobenzene in water. Sep Purif Technol. 2017;187:397-406. DOI: 10.1016/j.seppur.2017.05.030.
[32] Yang S, Li L, Xiao T, Zheng D, Zhang Y. Role of surface chemistry in modified ACF (activated carbon fiber)-catalyzed peroxymonosulfate oxidation. Appl Surf Sci. 2016;383:142-50. DOI: 10.1016/j.apsusc.2016.04.163.
[33] Zhu Y, Qiu S, Deng F, Ma F, Li G, Zheng Y. Three-dimensional nickel foam electrode for efficient electro-Fenton in a novel reactor. Environ Technol. 2018;0(0):1-36. DOI: 10.1080/09593330.2018.1509890.
[34] Jeon EK, Ryu S, Park SW, Wang L, Tsang DCW, Baek K. Enhanced adsorption of arsenic onto alum sludge modified by calcination. Elsevier Ltd. 2018; 176. DOI: 10.1016/j.jclepro.2017.12.153.
[35] Yang Y, Ma C, He X, Li J, Li M, Wang J. Calcined aluminum sludge as a heterogeneous Fenton - like catalyst for methylene blue degradation by three-dimensional electrochemical system. Electrocatalysis. 2021;12:698-714. DOI: 10.1007/s12678-021-00684-5.
[36] Thawini HH, Salman RH, Abdul-Majeed WS. Performance of electro-Fenton process for phenol degradation using nickel foam as a cathode. Iraqi J Chem Petrol Eng. 2023;24(3):13-25. DOI: 10.31699/ijcpe.2023.3.2.
[37] Lindner A, Radinger H, Scheiba F, Ehrenberg H. Structure-activity correlation of thermally activated graphite electrodes for vanadium flow batteries. RSC Adv. 2022;12(22):14119-26. DOI: 10.1039/d2ra02368g.
[38] Özkul E, Karabacakoğlu B. Removal of Sumifix Yellow EXF reactive azo dye by electro-Fenton method. J Turkish Chem Soc Sect A Chem. 2023;10(3):719-28. DOI: 10.18596/jotcsa.1226203.
[39] Mcyotto F, Wei Q, Macharia DK, Huang M, Shen C, Chow CWK. Effect of dye structure on color removal efficiency by coagulation. Chem Eng J. 2020;405:126674. DOI: 10.1016/j.cej.2020.126674.
[40] Rubi RVC, Olay JG, Caleon PBG, De Jesus RAF, Indab MBL, Jacinto RCH, et al. Photocatalytic degradation of diazinon in g-C3N4/Fe(III)/Persulfate system under visible LED light irradiation. Appl Sci Eng Process. 2021;14(1):100-7. DOI: 10.14416/j.asep.2020.12.008.
[41] Zhou L, Li J, Li F, Meng Q, Jing L, Xu X. Energy consumption model and energy efficiency of machine tools: a comprehensive literature review. J Clean Prod. 2015. DOI: 10.1016/j.jclepro.2015.05.093.
[42] Theydan SK, Mohammed WT. An electrocoagulation process operated at batch recirculation mode for treatment of refinery wastewaters: Optimization via response surface methodology. Egypt J Chem. 2022;65(131):1361-72. DOI: 10.21608/EJCHEM.2022.146203.6361.
[43] Henson RN. Analysis of Variance (ANOVA) In: Toga AW, editor. Brain Mapping. Academic Press; 2015:477-81. ISBN: 9780123973160. DOI: 10.1016/B978-0-12-397025-1.00319-5.
[44] Hameed ZM, Salman RH. Optimizing methyl orange degradation via electro-Fenton with copper foam cathode: A comparative approach using iron waste vs. iron salts and exploring catalyst and cathode durability. Appl Sci Eng Process. 2025;18(4):7728. DOI: 10.14416/j.asep.2025.05.002.
[45] Demirel C, Kabutey A, Herák D, Sedlaček A, Mizera Č, Dajbych O. Using Box-Behnken design coupled with response surface methodology for optimizing rapeseed oil expression parameters under heating and freezing conditions. Processes. 2022;10(3). DOI: 10.3390/pr10030490.
[46] Hameed ZM, Salman RH. Elimination of methyl orange dye with three dimensional electro-Fenton and sono-electro-Fenton systems utilizing copper foam and activated carbon. Ecol Eng Environ Technol. 2024;25(10):44-59. DOI: 10.12912/27197050/191199.
[47] Al-Khafaji RQ, Mohammed AHAK. Optimization of continuous electro-Fenton and photo electro-Fenton processes to treat Iraqi oilfield produced water using surface response methodology. IOP Conf Ser Mater Sci Eng. 2019;518(6). DOI: 10.1088/1757-899X/518/6/062007.
[48] Dolatabadi M, Świergosz T, Ahmadzadeh S. Electro-Fenton approach in oxidative degradation of dimethyl phthalate - The treatment of aqueous leachate from landfills. Sci Total Environ. 2021.772. DOI: 10.1016/j.scitotenv.2021.145323.
[49] Ghoneim MM, El-Desoky HS, Zidan NM. Electro-Fenton oxidation of Sunset Yellow FCF azo-dye in aqueous solutions. Desalination. 2011;274(1-3):22-30. DOI: 10.1016/j.desal.2011.01.062.
[50] Mahmud HNME, Huq AKO, Yahya RB. Removal of heavy metal ions from wastewater/aqueous solution by polypyrrole-based adsorbents: A review. RSC Adv. 2016;6:14778-91. DOI: 10.1039/C5RA24358K.